

# Investigating Active Sampling for Hardness Classification with Vision-Based Tactile Sensors

Junyi Chen<sup>1</sup>, Alap Kshirsagar<sup>1</sup>, Frederik Heller<sup>1</sup>, Mario Gómez Andreu<sup>1</sup>, Boris Belousov<sup>2</sup>, Tim Schneider<sup>1</sup>, Lisa P. Y. Lin<sup>3</sup>, Katja Doerschner<sup>3</sup>, Knut Drewing<sup>3</sup> and Jan Peters<sup>1,2,4,5</sup>

**Abstract**—One of the most important object properties that humans and robots perceive through touch is hardness. This paper investigates information-theoretic active sampling strategies for sample-efficient hardness classification with vision-based tactile sensors. We evaluate three probabilistic classifier models and two model-uncertainty-based sampling strategies on a robotic setup as well as on a previously published dataset of samples collected by human testers. Our findings indicate that the active sampling approaches, driven by uncertainty metrics, surpass a random sampling baseline in terms of accuracy and stability. Additionally, while in our human study, the participants achieve an average accuracy of 48.00%, our best approach achieves an average accuracy of 88.78% on the same set of objects, demonstrating the effectiveness of vision-based tactile sensors for object hardness classification.

## I. INTRODUCTION

Robots are increasingly being utilized in a variety of fields, from manufacturing to healthcare, where they interact with objects in their environment and plan their actions based on sensory feedback. A significant challenge in robotics is accurately perceiving object properties. This work focuses on a crucial property perceived through touch: *hardness*. Specifically, we investigate active sampling strategies for rapid hardness classification with a Vision-Based Tactile Sensor (VBTS). VBTSs like GelSight Mini [1] or FingerVision [2] provide a cost-effective and high-resolution alternative to traditional tactile sensors and also allow leveraging advancements in camera technology and computer vision. The ability to rapidly classify an object’s hardness can help robots in various tasks like waste sorting, automated harvesting, and handling delicate objects.

Several approaches have been proposed for robotic hardness classification as well as hardness prediction. For data collection, these methods rely on deformation measurements by cameras [3], force and torque sensors [4], or VBTS like *GelSight* [5]. To predict or classify the hardness based on the sensor measurements, traditional methods used analytical models based on physical rules [4], heuristics [3], or simple machine learning models like SVM and shallow neural networks [6]. In recent years, deep learning models like Convolutional Neural Networks (CNN) have become more preva-

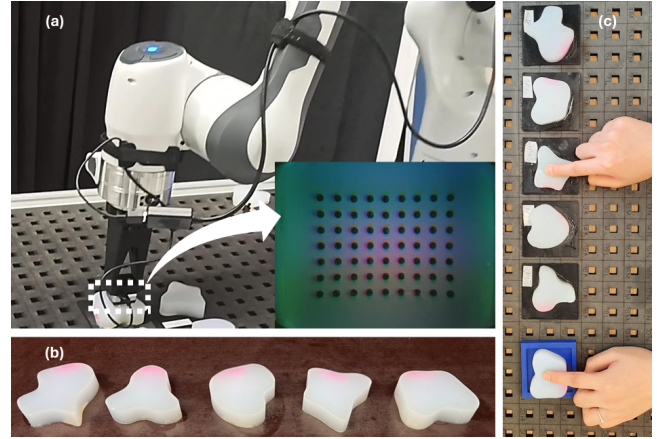


Fig. 1. The hardness classification task requires the agent to classify the test object into one of the reference classes based on hardness level. (a) The robot uses a GelSight Mini sensor mounted on its end-effector to explore the hardness of objects. The image captured by the sensor is shown in the inset. (b) Our dataset consists of GelSight Mini videos collected from five silicone objects of different shapes in increasing hardness from left to right. (c) In our human participant study, participants explored the test object (blue plate) and the reference objects (black plates) with their index fingers to compare hardness.

lent. These models can process high-dimensional data from high-resolution VBTSs and provide more accurate hardness assessments. Both classification [7]–[9] and regression [5], [10], [11] models have been proposed in the past. The regression models require true measurements of the hardness values (for example, with a Shore durometer), which is costly and time-consuming. In contrast, classification models do not require the exact hardness values and avoid measurement bias. Also, classification models can generalize well with fewer training samples. Therefore, in this work, we focus on the task of robotic hardness classification.

The existing hardness classification methods use a fixed number of samples collected from the training classes without regard for sample efficiency. In this work, we explore information-theoretic active sampling strategies for sample-efficient hardness classification. The robot is asked to classify a “test object” into one of the reference classes, based on the hardness level, with as few touches of a VBTS as possible (see Fig. 1). The robot has no prior knowledge about the objects and can collect multiple samples by touching the test and reference objects. Previously, Boehm et al. [12] investigated active sampling strategies for texture recognition with a VBTS. While Boehm et al. formulated texture recognition with a VBTS as an image classification problem, hardness

<sup>1</sup>Intelligent Autonomous Systems Lab, Department of Computer Science, TU Darmstadt, Germany. alap@robot-learning.de

<sup>2</sup>German Research Center for AI (DFKI)

<sup>3</sup>Department of Psychology, University of Giessen, Germany

<sup>4</sup>Centre for Cognitive Science, TU Darmstadt

<sup>5</sup>Hessian Center for Artificial Intelligence (Hessian.AI), Darmstadt

We thank Hessisches Ministerium für Wissenschaft & Kunst for the DFKI grant and “The Adaptive Mind” grant.

classification with a VBTS requires processing a sequence of frames [8], [9] and is more challenging as demonstrated in our work.

We provide new empirical evidence on the effectiveness of model-uncertainty-based active sampling strategies for hardness classification with a VBTS. We first compare three probabilistic classifier architectures on two datasets: our dataset containing videos collected by a robot pressing a GelSight Mini sensor on five silicone objects of different hardness levels (see Fig. 1) and the dataset created by Yuan et al. [5] containing videos obtained by human testers pressing an older version of the GelSight sensor on different silicone objects. Then, we implement two active sampling strategies with the most promising model for each dataset and compare them with a random sampling baseline. We also conduct a human-participant study to assess the performance of our method vis-à-vis human performance on the hardness classification task.

In the next sections, we present our hardness classification method, including the classifier model architectures and model-uncertainty-based active sampling strategies, followed by the experimental results on the two datasets and a human-participant study with objects in our dataset.

## II. METHOD

We seek to investigate sample-efficient hardness classification using vision-based tactile sensors. The agent first collects initial samples from each reference object and trains a probabilistic classifier on these samples. Then, the agent must decide which reference object to touch next to collect more samples and improve the classification accuracy. We use the uncertainty of the classifier for this decision. Our training algorithm is presented in Algorithm 1. In this section, we describe the method to choose input sequences for the classifiers, three architectures of the probabilistic classifiers, and three active sampling strategies.

### A. Classifier Input

When a VBTS like the *GelSight Mini* [1] is pressed against a deformable object, the changes in the color intensity of the image and the displacement of embedded markers (see Fig. 1) on the gelpad can be used for classifying the object’s hardness. The videos recorded from VBTS during the pressing motion encode temporal information as well. We constrain the input to the classifiers to the loading period of the press, i.e., from the point of initial contact to the point of maximum deformation. This helps to make the methods robust to the pressing motion’s speed and the maximum contact force. First, we subtract the initial frame in the video sequence from all the frames to account for any preexisting deformations in the elastomer. We determine the initial contact point by identifying the first frame where the mean intensity of the image is beyond a threshold and the last frame as the frame where the intensity reaches its peak. We select multiple additional frames between the first and last frames at equal intervals. This method has been shown

to be effective for hardness estimation with VBTS by Yuan et al. [5].

### B. Model Architectures

We implement three different probabilistic classifier architectures (see Fig. 2) for the task of hardness classification from VBTS videos. In each architecture, we use dropout layers to estimate the classifier’s uncertainty, allowing us to generate a distribution of predictions for each reference class. By randomly deactivating a subset of neurons during inference, dropout effectively simulates an ensemble of models, providing a measure of the network’s uncertainty [13].

*Model 1 – Optical Flow Features and Neural Network Classifier (OFNN):* This model is designed to classify video data by leveraging key motion features. Because object hardness influences the way the gel deforms when it is pressed against the object, optical flow features help capture these deformations by tracking motion patterns in the video. The model uses the most important 500 Lukas-Kanade [14] features extracted from the video frames as input. Then, it uses a 2-layer Neural Network (NN) with 128 neurons in the hidden layer, followed by a dropout layer, to classify the object’s hardness.

*Model 2 – DINOv2 Features and Neural Network Classifier (DINOv2NN):* This model consists of a self-supervised vision foundation model *DINOv2* [15] that extracts versatile visual features from images. We concatenate the features extracted from the frames in a VBTS video. Then, we feed these concatenated features to a simple two-layer neural network classifier, with 128 neurons in the hidden layer followed by a dropout layer similar to *OFNN*. We use a pre-trained *DINOv2-S/14* backbone and only update the weights of the NN classifier during training.

*Model 3 – Convolutional Long-Short Term Memory Network (ConvLSTM):* This architecture, proposed by Shi et al. [16], combines the strengths of CNN and Long Short Term Memory (LSTM) Network. The CNN layers extract spatial features from each frame, while the LSTM component learns and retains temporal relationships. A similar architecture was used in previous works [5], [11]. Our implementation of the model consists of 4 Convolutional Long Short Term Memory (ConvLSTM) layers with 4, 8, 14, and 16 filters and a dropout layer after each ConvLSTM layer. We train the model end-to-end on the VBTS videos to classify the object’s hardness without needing a separate feature extraction step.

### C. Active Sampling Strategies

The agent first trains the classifier model on a small number of initial samples collected from the reference objects (5 per object in our experiments). Following this initial training, the agent decides on the next reference object to collect more samples based on the model’s uncertainty. The agent queries the model repeatedly with the same test samples and estimates the model’s uncertainty from the distribution of the predictions generated due to the dropout layers. Similar

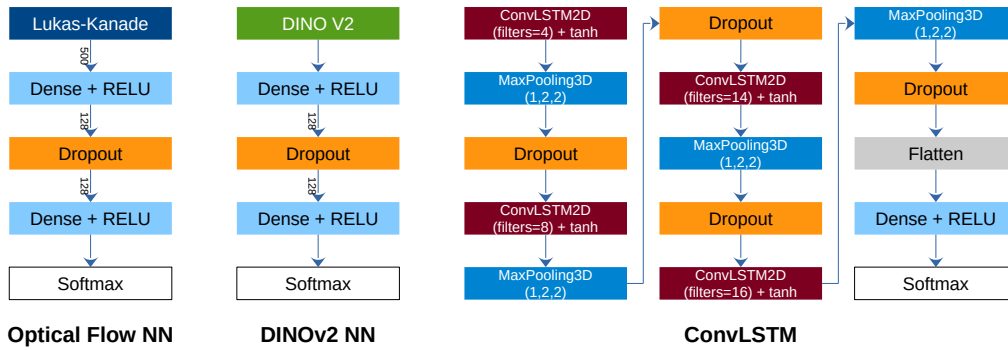


Fig. 2. The model architectures of *OpticalFlowNN*, *DINOv2NN* and *ConvLSTM*.

to Boehm et al. [12], we compare two uncertainty metrics—*entropy* and *variance*—obtained from the classifier’s predictions on the samples collected from the test object.

The entropy expectation of a class  $i$  is given by:

$$H_i = -\mathbb{E}_{j,k}(p_{i,j,k} \log(p_{i,j,k})) = -\frac{1}{nl} \sum_{k=1}^l \sum_{j=1}^n (p_{i,j,k} \log(p_{i,j,k})), \quad (1)$$

where  $p_{i,j,k}$  is the probability of the model classifying sample  $k \in \{1, \dots, l\}$  in the test set as class  $i$  in the  $j$ -th query ( $i \in \{1, \dots, m\}; j \in \{1, \dots, n\}$ ).

Similarly, variance is defined as

$$\text{Var}_i = \mathbb{E}_{j,k}(p_{i,j,k} - \mu_i)^2 = \frac{1}{nl} \sum_{k=1}^l \sum_{j=1}^n (p_{i,j,k} - \mu_i)^2, \quad (2)$$

where  $\mu_i$  is the mean of the  $n$  predictions of class  $i$ , given by,

$$\mu_i = \frac{1}{nl} \sum_{k=1}^l \sum_{j=1}^n p_{i,j,k} \quad (3)$$

The agent selects the reference class with the highest uncertainty and collects more samples from that class to refine the classifier model. As a baseline, we implement a *random* sampling strategy, in which the agent selects the next reference class randomly from a uniform distribution.

#### D. Retraining with Reservoir Sampling

To manage the size of the training data, we employ reservoir sampling to select a subset of samples from the growing dataset. The agent adds newly collected reference samples to the training reservoir and retrains the classifier model using the updated training reservoir. If the size of the training reservoir exceeds a predefined threshold  $M$ , the agent randomly selects a subset of size  $M$  from the reservoir for training. Otherwise, the agent uses all available samples for training.

### III. EVALUATION

We seek to evaluate the effectiveness of active sampling strategies for the hardness classification task and also compare their performance with human performance. To do so,

---

#### Algorithm 1 Hardness classification with active sampling

---

- 1: **Input:** Base classes  $B$ ; Initial samples per class  $s_0$ ; Initial training epochs  $e_0$ ; Active sampling iterations  $N$ ; Strategy  $S \in \{\text{“entropy”}, \text{“variance”}, \text{“random”}\}$ ; New samples introduced to the reservoir per iteration per class  $s$ ; Maximum samples per training iteration  $M$ ; Training epochs per iteration  $e$ ; Predictions per test sample to estimate model uncertainty  $n$ ; Training reservoir  $TR$ ; Training samples  $TS$
  - 2: **Output:** Trained classifier model
  - 3: Initialize  $TR$  with  $s_0$  samples from each class in  $B$
  - 4: Train the model for  $e_0$  epochs using  $TR$
  - 5: **for**  $i = 1$  to  $N$  **do**
  - 6:   Make  $n$  predictions on  $l$  test samples with dropout
  - 7:   **if**  $S = \text{“entropy”}$  **then**
  - 8:     Calculate the entropy of predictions (Eq. 1)
  - 9:      $selected\ class \leftarrow$  class with highest entropy
  - 10:   **else if**  $S = \text{“variance”}$  **then**
  - 11:     Calculate the variance of predictions (Eq. 2)
  - 12:      $selected\ class \leftarrow$  class with highest variance
  - 13:   **else if**  $S = \text{“random”}$  **then**
  - 14:      $selected\ class \leftarrow$  random class from  $B$
  - 15:   **end if**
  - 16:   Add  $s$  samples from  $selected\ class$  to  $TR$
  - 17:   **if** size of  $TR > M$  **then**
  - 18:      $TS \leftarrow$  randomly select  $M$  samples from  $TR$
  - 19:   **else**
  - 20:      $TS \leftarrow TR$
  - 21:   **end if**
  - 22:   Train the model with  $TS$  for  $e$  epochs
  - 23: **end for**
- 

we first evaluate the three classifier models from Sec. III-D on our dataset and a previously published dataset. Then, we test the active sampling strategies with the best model for each dataset. Finally, we conduct a human-participant study to estimate the hardness classification accuracy of humans on the objects in our dataset.

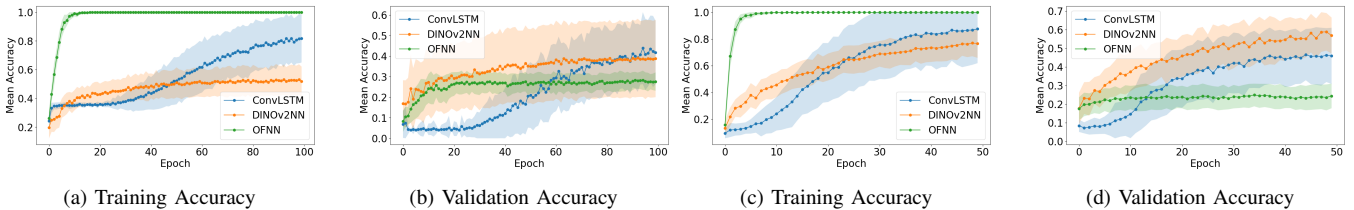


Fig. 3. Training and validation accuracies of the classifier models (see Sec. II-B) on our dataset (a and b) and the Yuan dataset (c and d) (see Sec. III-A). The accuracies are averaged over 50 runs and 90 runs, respectively, for the two datasets.

## A. Datasets

We tested our hardness classification method on two datasets: a dataset that we created containing five hardness classes and a dataset created by Yuan et al. [5] containing nine hardness classes.

1) *Our Dataset*: We created a set of objects, shown in Fig. 1, of five different hardness levels by mixing a two-component silicone rubber solution (Alpa Sil EH A and B) with different amounts of silicone oil. The resulting hardness levels were - (least hard) 1.13 mm/N; 1.02 mm/N; 0.79 mm/N; 0.68 mm/N; 0.44 mm/N (hardest). We used 3D-printed molds to cast the objects, ensuring flat surfaces free of air pockets and any noticeable texture differences.

To collect data of the robot exploring the hardness of these objects, we mounted a *GelSight Mini* [1] tactile sensor on the end effector of a Franka Emika *Panda* 7-DOF robot arm. The robot pushed the tactile sensor on the top surface of each object, as shown in Fig. 1, with a given velocity ( $v_{\text{push}}$ ) and retreated when the contact force reached a given threshold ( $F_{\text{push}}$ ), while recording videos from the sensor’s internal camera. The contact force, estimated from the robot’s joint torque sensors, was used solely for data collection and not for hardness classification. The robot always pushed the sensor in the center of the object so that it did not capture any edges, and there was no influence of the shape of the sample on the hardness classification performance.

Each video represents one data point in our dataset, and there are a total of 455 recordings in the dataset. To increase variance in the data, the maximum contact force and the downward velocity of the end-effector ( $v_{\text{push}}$ ) were randomly sampled from uniform distributions with  $F_{\text{push}} \in [1\text{N}, 5\text{N}]$  and  $v_{\text{push}} \in [20\text{mms}^{-1}, 50\text{mms}^{-1}]$ . Each captured video is labeled with its hardness class  $\in \{1, \dots, 5\}$ . The dataset also contains the contact force between the *GelSight* sensor and the object, measured by the robot’s F/T sensors, as well as a timestamp for each frame in the videos. Our dataset is available at: <https://archimedes.ias.informatik.tu-darmstadt.de/s/PrXF7P48tAJnTqL>.

We apply the procedure described in Sec. II-A to select the input frames for the classifier from each video. We use a threshold of 1400 to identify the first frame of contact and select two additional frames between the first and the last frame at equal intervals.

2) *Yuan Dataset*: Yuan et al.’s [5] dataset comprises approximately 7,000 videos, each representing an independent pressing sequence where human testers press the *GelSight*

sensor onto various silicone samples. In our experiments, we focus on the “flat” object category from the dataset with 11 different hardness levels on the Shore 00 scale: 8, 11, 17, 27, 46, 48, 62, 73, 81, 87, and 95. Since the difference between the hardness levels of some classes is very small, we remove classes 48 and 11 so that the minimum difference between classes is 6. The remaining classes have hardness levels 8, 17, 27, 46, 62, 73, 81, 87, and 95 on the Shore 00 scale. We select only one additional frame between each video’s initial and final frame of contact to ensure at least 10 samples per object,

## B. Hyperparameters

We set the number of initial samples collected from each reference object and the number of new samples collected in each iteration to five. We found that the samples in our dataset were much harder to classify than the samples in the Yuan dataset (see Fig. 3). Therefore, for our dataset, we set the number of initial training epochs to 100, with 50 additional epochs per active sampling iteration. For the Yuan dataset, we set the initial training epochs to 50, with 25 additional epochs per active sampling iteration. Due to GPU memory constraints, we restricted the number of training samples selected from the reservoir per iteration to 80 for the OFNN and DINOv2NN models and 40 for the ConvLSTM model which required significantly more GPU memory due to its architecture.

## C. Evaluation Metrics

After the initial training, we evaluate the model’s accuracy on test samples with the dropout layer disabled during inference. We also assess the model’s accuracy after each active sampling iteration to monitor its performance throughout the active sampling process. In practical applications, our model operates as a classifier rather than a regressor, making it agnostic to the specific hardness metric of the samples. Nevertheless, even if the model misclassifies the hardness level, it is preferable to predict a class with a hardness level closer to the true value. Therefore, alongside accuracy, we compute the Mean Absolute Error (MAE) between the predicted and actual hardness values to assess the model’s pseudo-regression and ordinal classification capabilities of quantifying the hardness level.

## D. Model Baselines

We first compare the performance of the three classifier models—OFNN, DINOv2NN, and ConvLSTM—trained with

the initial samples without any active sampling on both datasets. Each model is trained on five samples per class and evaluated on five validation samples per class. As described in Sec. III-A, our dataset has five classes, whereas the Yuan dataset has nine classes. Fig. 3 shows the training and validation accuracies of the models averaged over 10 runs per class. We find that *ConvLSTM* outperforms the other two models on our dataset, achieving a validation accuracy of 42%, *DINOv2NN* follows close behind with an accuracy of 38%, and *OFNN* performs the worst with a validation accuracy of only 27%. On the Yuan dataset, *DINOv2NN* outperforms the other two models, achieving a validation accuracy of 59%, *ConvLSTM* is next with an accuracy of 46%, and *OFNN* performs the worst with a validation accuracy of only 24%.

### E. Effects of Dropout Rate

As described in Sec II-B, we use dropout layers to estimate the model uncertainty. If the dropout rate is too high, the uncertainty evaluation procedure may suffer from randomness and subsequent inability to estimate the model uncertainty. To test the effect of different dropout rates, we evaluated the performance of *DINOv2NN* model on the Yuan dataset with different dropout rates ranging from 0.05 to 0.5. The model is trained on 5 samples per class and evaluated on 5 validation samples per class. Fig. 4 shows the mean accuracy and MAE for 9 runs. We find that a dropout rate higher than 0.2 causes a significant degradation in the performance and stability of the model. Therefore, in our evaluation of the active sampling strategies we use a dropout rate of 0.2.

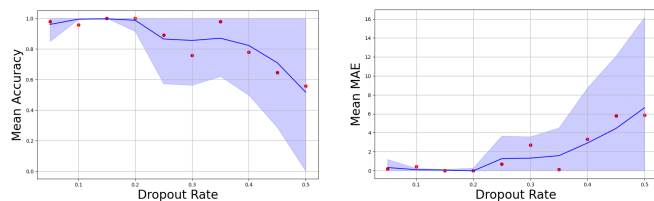


Fig. 4. Mean test class accuracy and MAE, and their corresponding standard deviation over different dropout rates of *DINOv2NN* model on the Yuan Dataset. Savitzky-Golay filter is used to smooth the data points for visualization purposes.

### F. Active Sampling Performance

We test both information-theoretic active sampling strategies (*entropy* and *variance*) and compare them to the *random* sampling baseline on our dataset and the Yuan dataset, with the best-performing classifier models, i.e., *ConvLSTM* for our dataset and *DINOv2NN* for the Yuan dataset.

1) *Our Dataset*: The *ConvLSTM* model is initially trained on 5 samples per class, and then we run the active sampling algorithm for 5 iterations. We add 5 samples from the selected class in each iteration. The results are averaged over 5 comparison classes, where each class is replicated with 10 runs. Therefore, there are 50 runs for each strategy.

We observed that in 122 out of 150 runs (81.33%) of *ConvLSTM* on our dataset, the model converged, whereas,

on the remaining runs, the model diverged, always predicted a certain class regardless of the input. This is likely due to the complexity of *ConvLSTM*, which caused it to require more training samples to converge. We observed that a training loss greater than 1, after training on the initial samples, indicated divergence for a *ConvLSTM* model. Therefore, if the training loss exceeded 1, we considered the model to have failed to converge and did not run active sampling on it.

Fig. 5 shows the mean accuracy and mean MAE, and Fig. 6 shows the entropy and variance for the three strategies on our dataset. We find that both the active sampling strategies outperform the baseline *random* strategy, with the *variance* strategy performing better than the *entropy* strategy in most active sampling iterations.

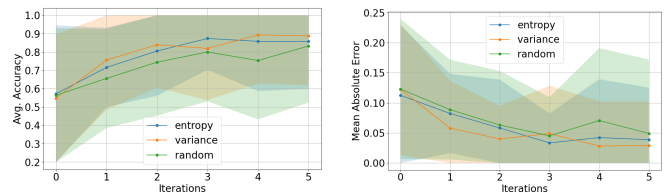


Fig. 5. Comparison of the classification accuracies and MAEs for the three strategies on our dataset. The shaded area indicates the standard deviation. In most iterations, the *variance* strategy achieves the highest accuracy and lowest MAE, closely followed by the *entropy* strategy.

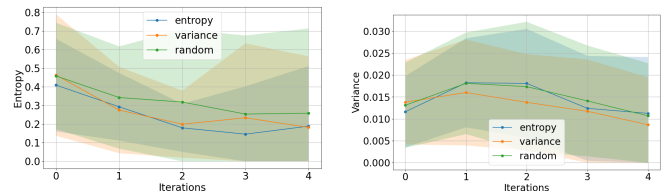


Fig. 6. Comparison of the mean entropy and variance for the three strategies on our dataset. Both *entropy* and *variance* strategies lead to a comparable decrease in the entropy in most iterations. However, the *variance* strategy results in the lowest variance as compared to the other two strategies.

2) *Yuan's Dataset*: The *DINOv2NN* model is initially trained on 5 samples per class, and then we run the *active sampling* algorithm for 5 iterations. We add 5 samples from the selected class in each iteration. The results are averaged over 9 comparison classes, where each class is replicated with 5 runs. Therefore, there are 45 runs for each strategy. We did not observe any convergence issues with the *DINOv2NN* model on the Yuan dataset.

Fig. 7 shows the mean accuracy and mean MAE and Fig. 8 for the three strategies on the Yuan dataset. We find that both the active sampling strategies outperform the baseline *random* strategy, with the *variance* strategy performing better than the *entropy* strategy in most active sampling iterations.

### G. Human Study

We conducted a human-participant study to investigate the human performance of hardness classification with the objects in our dataset. We recruited ten participants from the university's student population for the study. Participants

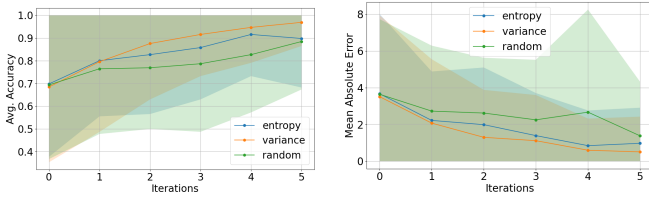


Fig. 7. Comparison of the classification accuracies and MAEs for the three strategies on the Yuan dataset. The shaded area indicates the standard deviation. In most iterations, the *variance* strategy achieves the highest accuracy and lowest MAE, closely followed by the *entropy* strategy.

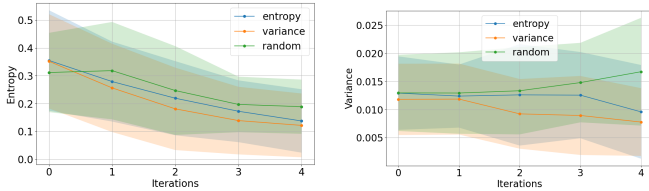


Fig. 8. Comparison of mean entropy and variance for the three strategies on the Yuan dataset. The *variance* strategy results in the lowest entropy and the lowest variance in each active sampling iteration.

reported no issues with their tactile perception ability. Each experiment trial consisted of a practice round and five test rounds. In each round, participants were asked to find one of five reference objects with the same hardness level as the test object. The participants were blindfolded and allowed to press the objects only with their index fingers to keep the setup similar to the robotic setup (see Fig. 1). The participants pressed the test object with their left index finger while exploring the reference objects with their right index finger. Each round had a time limit of 30 seconds, within which the participants had to explore all five reference objects and classify the test object, but the participants could end the round earlier by verbally confirming their choice of the reference object. In each of the five test rounds per participant, we used a different test object from our dataset (see Sec. III-A.1) and shuffled the sequence of the five reference objects. We found that the average classification accuracy of the participants was 48% with a standard deviation of 22%. As shown in Table I, the ConvLSTM classifier outperforms the human participants, both with and without the active sampling strategies, on the same set of objects.

TABLE I  
HARDNESS CLASSIFICATION ACCURACIES ON OUR DATASET.<sup>1</sup>

<i>Humans</i>	<i>No Resampling</i>	<i>Variance</i>	<i>Entropy</i>	<i>Random</i>
48.00%	57.20%	<b>88.78%</b>	85.79%	83.26%
±22.27%	±37.25%	±26.85%	±25.85%	±30.84%

We annotated experiment videos with the positions of the fingers and objects, using a custom semi-automatic pipeline

<sup>1</sup>*Humans* denotes the accuracy of the human participants in our study (see Sec. III-G). *No Resampling* denotes the accuracy of the ConvLSTM classifier with five initial samples per class (see Sec. III-D). For the three active sampling strategies, the accuracies shown are after 5 sampling iterations.

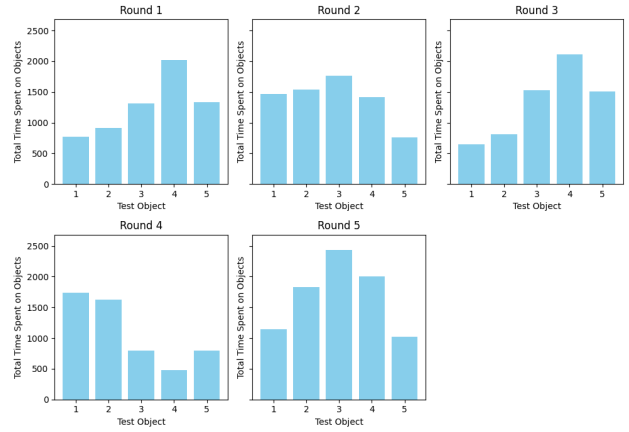


Fig. 9. Total time of all participants spent on each test object for each round. Participants focused more on the correct object (4, 2, 5, 1, 3 for 1 - 5 rounds, respectively) or objects with similar hardness.

consisting of MediaPipe [17] and Segment Anything Model-2 [18]. We counted the duration in which the right index finger remained on a test object. As shown in Fig. 9, participants spent more time on objects with similar hardness to the correct one while paying less attention to others. Also, they often struggled to distinguish similar hardness levels and selected an incorrect but similarly hard object.

## IV. DISCUSSION

We investigated the performance of a model-uncertainty-based approach to active sampling for hardness classification with a VBTS. We evaluated different classifier architectures, dropout rates, and active sampling strategies to find out the choices that maximize classification accuracy.

First, we compared three model architectures for the task of hardness classification, without any active sampling, on two datasets of VBTS videos collected from objects of different hardness levels. We found that the best hardness classifiers achieved accuracies of 42% and 59% with five training samples per class on the two datasets, respectively. (see Fig. 3). Whereas in the texture recognition task of Boehm et al. [12], the classifier achieved 80% accuracy even with just one sample per class. Also, in contrast to the findings of Boehm et al., where rotation-based data augmentation greatly improved the model performance, we found that rotation-based data augmentation techniques are ineffective. These results suggest that hardness classification is more difficult than texture recognition for a VBTS. Therefore, it warrants an investigation of the active sampling strategies from [12] for the task of hardness classification.

Second, we investigated two active sampling strategies aimed at maximizing information gain by selecting samples with higher model uncertainty. We found that the *variance* strategy achieved the highest accuracy and the lowest MAE from the ground truth as compared to the *entropy* strategy and a random sampling baseline on both datasets and significantly reduced the standard deviation of those metrics (see Fig. 5 and 7). The plots of variance and entropy (Fig. 6

and Fig. 8) offer some explanation: as the model learns from more samples, every strategy, including the random baseline, shows a decrease in the entropy. In contrast, reducing the variance is much harder, and the *variance* strategy reduces it most effectively. Our results demonstrate that the active sampling strategies can guide the model in selecting the most informative samples, enhancing hardness classification accuracy as compared to a random sampling baseline.

Third, we conducted a human-participant experiment to compare the accuracy of our VBTS-based hardness classification approaches to the accuracy of humans on the same set of objects. We found that a ConvLSTM classifier trained on 5 VBTS samples per class achieved a 10% higher accuracy than the average accuracy of human participants in our experiments. Furthermore, with 5 active sampling iterations of 5 samples each, the classifier's accuracy improved by 40% than the average human accuracy. The low accuracy in human hardness classification can be attributed to the similar hardness values of the tested objects. While we recognize the differences in tactile perception between humans and VBTS, our findings demonstrate the effectiveness of VBTS-based hardness classification compared to humans.

*Limitations and Future Work:* Our experiments only considered on the hardness classification of flat objects, whereas several real-world hardness classification tasks involve complex object shapes. Also, the robot and the human participants were restricted to single-finger explorations of the objects. Finally, though our results show that the active sampling strategies improved the model's classification accuracy on average, the variation in the model's performance remains high. Future works could focus on sample-efficient hardness classification of complex objects with multi-modal data such as proprioceptive, visual, and tactile data. Another direction of future work can investigate human-inspired active sampling as well as active exploration strategies with single and multi-fingered grippers.

## REFERENCES

- [1] "GelSight Mini System - GelSight," April 2023, [Online; accessed 15. Sept. 2024]. [Online]. Available: <https://www.gelsight.com/product/gelsight-mini-system>
- [2] A. Yamaguchi and C. G. Atkeson, "Recent progress in tactile sensing and sensors for robotic manipulation: can we turn tactile sensing into vision?" *Advanced Robotics*, vol. 33, no. 14, pp. 661–673, 2019.
- [3] F. Pallottino, C. Costa, P. Menesatti, and M. Moresi, "Assessment of the mechanical properties of tarocco orange fruit under parallel plate compression," *Journal of Food Engineering*, vol. 103, pp. 308–316, April 2011.
- [4] M. Burgess, "Learning object compliance via young's modulus from single grasps with camera-based tactile sensors," *arXiv preprint arXiv:2406.15304*, 2024.
- [5] W. Yuan, C. Zhu, A. Owens, M. A. Srinivasan, and E. H. Adelson, "Shape-independent hardness estimation using deep learning and a gelsight tactile sensor," in *IEEE International Conference on Robotics and Automation*, July 2017, pp. 951–958.
- [6] Z. Zhang, J. Zhou, Z. Yan, K. Wang, J. Mao, and Z. Jiang, "Hardness recognition of fruits and vegetables based on tactile array information of manipulator," *Computers and Electronics in Agriculture*, vol. 181, p. 105959, 2021.
- [7] Y. Amin, C. Gianoglio, and M. Valle, "Embedded real-time objects' hardness classification for robotic grippers," *Future Generation Computer Systems*, vol. 148, pp. 211–224, November 2023.

- [8] S. Fang, T. Mi, Z. Zhou, C. Ye, C. Liu, H. Wu, Z. Yi, and X. Wu, "Tactcapsnet: Tactile capsule network for object hardness recognition," *IEEE International Conference on Real-Time Computing and Robotics*, pp. 1128–1133, July 2021.
- [9] S. Fang, Z. Yi, T. Mi, Z. Zhou, C. Ye, W. Shang, T. Xu, and X. Wu, "Tactonet: Tactile ordinal network based on unimodal probability for object hardness classification," *IEEE Transactions on Automation Science and Engineering*, vol. 20, pp. 2784–2794, 2023.
- [10] S. Nam, T. Jack, L. Y. Lee, and N. F. Lepora, "Softness prediction with a soft biomimetic optical tactile sensor," in *International Conference on Soft Robotics*, April 2024, pp. 121–126.
- [11] Y. Chen, J. Lin, X. Du, B. Fang, F. Sun, and S. Li, "Non-destructive fruit firmness evaluation using vision-based tactile information," in *International Conference on Robotics and Automation*, 2022, pp. 2303–2309.
- [12] A. Böhm, T. Schneider, B. Belousov, A. Kshirsagar, L. Lin, K. Dörschner, K. Drewing, C. A. Rothkopf, and J. Peters, "What matters for active texture recognition with vision-based tactile sensors," in *IEEE International Conference on Robotics and Automation*, 2024, pp. 15 099–15 105.
- [13] Y. Gal and Z. Ghahramani, "Dropout as a bayesian approximation: Representing model uncertainty in deep learning," *arXiv preprint arXiv:1506.02142*, 2016.
- [14] B. D. Lucas and T. Kanade, "An iterative image registration technique with an application to stereo vision," in *International Joint Conference on Artificial Intelligence*, vol. 2, 1981, pp. 674–679.
- [15] M. Oquab, T. Darcet, T. Moutakanni, H. Vo, M. Szafraniec, V. Khalidov, P. Fernandez, D. Haziza, F. Massa, A. El-Nouby *et al.*, "DINOv2: Learning robust visual features without supervision," *arXiv preprint arXiv:2304.07193*, 2023.
- [16] X. Shi, Z. Chen, H. Wang, D.-Y. Yeung, W.-K. Wong, and W.-c. Woo, "Convolutional LSTM network: A machine learning approach for precipitation nowcasting," *Advances in Neural Information Processing Systems*, vol. 28, 2015.
- [17] C. Lugaresi, J. Tang, H. Nash, C. McClanahan, E. Uboweja, M. Hays, F. Zhang, C.-L. Chang, M. G. Yong, J. Lee *et al.*, "Mediapipe: A framework for building perception pipelines," *arXiv preprint arXiv:1906.08172*, 2019.
- [18] N. Ravi, V. Gabeur, Y.-T. Hu, R. Hu, C. Ryal, T. Ma, H. Khedr, R. Rädle, C. Rolland, L. Gustafson *et al.*, "Sam 2: Segment anything in images and videos," *arXiv preprint arXiv:2408.00714*, 2024.